Int. J. Electrochem. Sci., 13 **(2018)** 563 – 586, doi: 10.20964/2018.01.51

International Journal of
ELECTROCHEMICAL
SCIENCE
www.electrochemsci.org

Enzymatic Electrochemical Biosensor Based on Multiwall Carbon Nanotubes and Cerium Dioxide Nanoparticles for Rutin Detection

Stephen Rathinaraj Benjamin[1,2], *Ramon Silva Vilela*[1,3], *Henrique Santiago de Camargo*[1], *Maria Izabel Florindo Guedes*[2], *Katia Flavia Fernandes*[3], *Flavio Colmati*[1,*]

[1] Laboratory of Bio-electrocatalysis and Fuel Cells (LABEL-FC), Instituto de Química, Universidade Federal de Goiás, IQ-UFG, Av. Esperança, s n. 74690-900 Goiânia – GO, Brasil.
[2] Grupo de Inovação Biotecnológica em Saúde, Laboratório de Biotecnologia e Biologia Molecular-LBBM, Universidade Estadual do Ceará (UECE), Av. Paranjana, 1700 - Campus do Itaperi – 60714-903 Fortaleza – CE Brasil.
[3] Laboratório de Química de Polímeros, Instituto de Ciências Biológicas, Departamento de Ciências Fisiológicas, Universidade Federal de Goiás (ICB-UFG), Av. Esperança, s n. 74690-900 Goiânia – GO, Brasil.
[*]E-mail: colmati@ufg.br

Received: 1 October 2017 / *Accepted:* 10 November 2017 / *Published:* 16 December 2017

In this study, a simple and sensitive enzymatic electrochemical biosensor was developed to detect rutin by cyclic voltammetry (CV), differential pulse voltammetry (DPV) and square wave voltammetry (SWV) using a carbon paste electrode modified with a multiwall carbon nanotube (MWCNT), cerium oxide nanoparticle (CeO_2), and crude extract source of peroxidase enzyme (POx) composite. The electrochemical parameters and experimental conditions were optimized and evaluated. The enzymatic electrochemical biosensor (CeO2/POx/MWCNTs/CPE) showed excellent electrocatalytic activity towards the detection of rutin. The surface physical characteristics of the modified electrode were studied by scanning electron microscopy (SEM) and transmission electron microscopy (TEM). This biosensor demonstrated selectivity, stability, and reproducibility, which was further applied to detect rutin in medicine tablets and capsules with recoveries in the range of 97-102%.

Keywords: Multiwall carbon nanotubes, Cerium dioxide nanoparticles, Crude extract, Rutin, POx.

1. INTRODUCTION

Flavonoids comprise a large family of naturally occurring organic compounds widely extended in the plant kingdom. These compounds are usually found in vegetables and fruits and constitute a significant part of the human diet [1]. Furthermore, flavonoids exhibit an extensive range of biological

activities such as coronary heart disease, cancers, anti-inflammatory, anti-atherogenic and antiviral activities [2]. Moreover, as demonstrated by García-Lafuente [3] and Benavent-Garci [4], some species of flavonoids exhibit potential antiviral activities. Rutin belongs to an essential type of bioflavonoids and is distributed in fruits and vegetables. Additionally, rutin reduces the cytotoxicity of oxidized low-density lipoprotein (LDL) and lowers the risk of heart disease [3-5].

In recent years, there have been many studies with different nanomaterials, for instance, carbon nanotubes in combination with a carbon paste electrode (referred to as a carbon nanotube paste electrode, CNTPE) have been extensively used in the preparation of sensors [6-12]. In comparison with most of the commercially available sensors, carbon nanotubes show remarkable properties such as chemical stability, high specific electrical conductivity, and high sensitivity due to its high surface area. [2, 13, 14].

Indeed, carbon nanotubes on an electrode surface have indicated phenomenal electrocatalytic reduction towards H_2O_2 (hydrogen peroxidase) and NADH, which can be assigned to the fast electron transferability of carbon nanotubes [12]. On the other hand, metal nanoparticles have also attracted considerable interest, in fields such as optics, catalysis, and electrocatalysis, because of their size- and shape-dependent physicochemical properties [15].

In addition, the combination of carbon nanotubes with metal oxide nanomaterials may be interestingly useful for enhancing optical and physical properties. Recently, cerium dioxide nanoparticles (CeO_2NPs) have attracted much interest in building amperometric biosensors owing to their high isoelectric point (IEP) (~9.0), biocompatibility, chemical stability, high oxygen storage capacity [15-17], etc.

Considering the excellent aspects of the CNT-metal oxide nanostructure-based biosensors, their utilization presents new opportunities to establish novel analytical biosensors based on the electron transfer reaction of redox enzyme devices with improved performance [18-21].

Several enzymes from the peroxidase family (E.C. 1.11.1) has been widely used for the selective measurement of phenols, and total polyphenolic contents in food and environmental matrices [22-24]. Additionally, these enzymes have been generally utilized as a part of the development of biosensors for phenolic and catecholic substrates, since these compounds have improved the rate of catalytic reduction of peroxidase in terms of transference among immobilized enzymes and electrodes [23, 25]. In the last case, the immobilization process of the enzyme on an electrode surface can be attributed to the oxidized configuration of the enzyme that is reduced to its native form by direct and/or mediated electron transfer [26, 27].

Nevertheless, it is well known that peroxidases can conduct direct electron transfer between enzyme molecules and an electrode surface.

When peroxidase is immobilized on an electrode surface, the oxidized form of the enzyme, which is formed in the reaction with peroxide, can be reduced to its native form by direct and/or mediated electron transfer by means of electron donating compounds, such as the phenol species [28]. The enzyme mechanism that occurs in a biosensor based on peroxidase consists of the oxidation of the enzyme by hydrogen peroxide, followed by its reduction with a given phenolic compound (rutin) [29].

The hydrogen peroxide and the electron-donating phenolic-derived compounds are included. At the electrode surface, the enzyme molecules are oxidized by hydrogen peroxide, followed by their

reduction by the phenolic compound. The sensitivity of these peroxidase-based biosensors is constrained by the high current due to the direct electron exchange between the enzyme and the electrode surface in the presence of hydrogen peroxide.

The observed reducing current is proportional to the phenolic compound concentration at electrode surface, as demonstrated below [24, 26, 27, 30]:

$$H_2O_2 + POx \rightarrow H_2O + POx_{ox}{}^{I} \quad (\mathbf{1})$$

$$POx_{ox}{}^{I} + AH_2 \rightarrow POx_{ox}{}^{II} + {}^{\cdot}AH \quad (\mathbf{2})$$

$$POx_{ox}{}^{II} + AH_2 \rightarrow POx_{red} + {}^{\cdot}AH + H_2O \quad (\mathbf{3})$$

$$2AH^{\cdot} + 2e + 2H^{+} \rightarrow 2AH_2 \quad (\mathbf{4})$$

Here, $POx_{ox}{}^{I}$ and $POx_{ox}{}^{II}$ are oxidized intermediate species of the enzyme POx, AH_2 is the reduced substrate (phenolic compounds) and ${}^{\cdot}AH$ is a free radical. In the first step, the enzyme is oxidized by hydrogen peroxide, resulting in an oxidized intermediate compound from the enzyme. This oxidized intermediate compound is reduced to its native form in two steps, as demonstrated in equations 2 and 3 [24, 26, 20-32]. The electrochemical step to observe the reduction current is presented in Eq. 4.

The peroxidases from *Cucurbita pepo L.* (Cucurbitaceae) and most of the oxidoreductases have a high affinity for natural phenolic compounds, which is illustrated by their lower potential of reduction. An amperometric biosensor was previously constructed by incorporating selected portions of *Cucurbita pepo L*. in a carbon paste electrode [33-35]. Among these remarkable principles, various phenolic and other electron-donor substances have been determined by peroxidase biosensors. In the present study, we immobilized the peroxidase from *Cucurbita pepo* (POx) onto a POx/CeO_2/MWCNTs/CPE electrode for the determination of rutin in pharmaceutical formulations. This system consists of enhancing the electron transfer between the enzyme and transductor by means of the intimate connection of the biological component with two nanomaterials: CNTs and CeO_2NPs, which have demonstrated an enhancement in the electrocatalytic performance of other different (bio) sensors [35-37]

The structural characterization of the electrode material has been conducted by using scanning electron microscopy (SEM) and transmission electron microscopy (TEM). Moreover, electrochemical characterizations have been carried out by using various electrochemical techniques such as cyclic voltammetry (CV), differential pulse voltammetry (DPV) and square wave voltammetry (SWV). The following figures of merits for this electrochemical enzymatic biosensor were calculated: limit of detection, linearity and the response time. Consequently, these studies show the electrochemical activity in terms of the direct electron transfer of the POx enzyme towards rutin sensing along with the proposed biosensing compatibility. Moreover, its application in real samples offered very satisfactory results.

2. MATERIALS AND METHODS

Multiwall carbon nanotubes (99.95%, <50 nm diameter, 1-2 µm length), nanopowder-based cerium (IV) dioxide (99.95%), high-purity mineral oil (Nujol®) and ethanol were purchased from

Sigma–Aldrich (St. Louis, MO USA). KH_2PO_4 and K_2HPO_4 for the phosphate buffer solution (PBS) were from Vetec Química, Fina Ltd. (Rio Janeiro, Brazil). Graphite powder (high-purity Ultracarbon®), Ultra F-purity was obtained from Bay City, MI, USA. Rutin in two different dosage forms (capsules and tablets) were obtained from a local pharmacy (Goiânia – GO, Brazil). The rutin content in the tablets and capsules were 500 mg and 40 mg, respectively. Stock solutions of rutin were freshly prepared by dissolving capsules or tablets in an appropriate amount of analytical grade methanol and stored until analysis at 5 °C in darkness. Daily diluted solutions were prepared from the stock solution. All electrolyte solutions were prepared by using high analytical grade salts, which were diluted in purified water (Milli-Q, Millipore S. A., Molsheim, France).

2.1 Preparation of the enzymatic crude extract

Healthy *zucchini* (*Cucurbita pepo)* used throughout this work were acquired from a farm in Goiânia - GO, Brazil. This cultivation area was exclusively used to collect the biological material, to always maintain similar characteristics of the product. After washing and drying, 25 g of peeled and chopped zucchini were homogenized in a blender containing 25 mL of 0.1 mol L^{-1} phosphate buffer (pH 7.0). Then, the homogenate was filtered through four layers of cloth (gauze) and centrifuged at 15,000 rpm for 20 min at 4 °C. The supernatant solution was divided into several aliquots and stored in a refrigerator at 4 °C and used as the enzyme source peroxidase. The remaining crude extracts were obtained using the same procedure [38, 39].

2.2 Determination of the activity and total protein content of the peroxidase enzyme

The activity of POx extracted from *Zucchini* tissues were assayed in triplicate by measuring the absorbance at 470 nm of the tetraguaiacol formed in the enzymatic reaction. In this determination, 0.2 mL of the homogenate containing POx was added to 2.7 mL of a 0.05 mol L^{-1} guaiacol solution, and both were prepared in a 0.1 mol L^{-1} phosphate buffer (pH 7.0) at 25 °C. The reaction was started by the addition of 0.1 mL of the 0.01 mol L^{-1} H_2O_2 solution. One unit of activity (unit: mL^{-1}) was defined as the amount of enzyme that causes an increase in 0.001 absorbance units per minute under the abovementioned conditions. The total protein content of the supernatant solution was determined by the Biuret method using bovine serum albumin as the standard.

2.3 POx biosensor construction

Figure 1 describes the basic strategy for the preparation of the POx biosensor. The biosensor was constructed by the addition and subsequent homogenization of the following reagents: carbon powder, POx crude extract, carbon nanotubes and cerium oxide nanopowder (CNP). Later, the mineral oil Nujol® was added to this mixture and mixed in a mortar for at least 20 min to produce the final paste. The CPE surface was first smoothed with clean paper until a shiny appearance was evident and then rinsed with doubly distilled water.

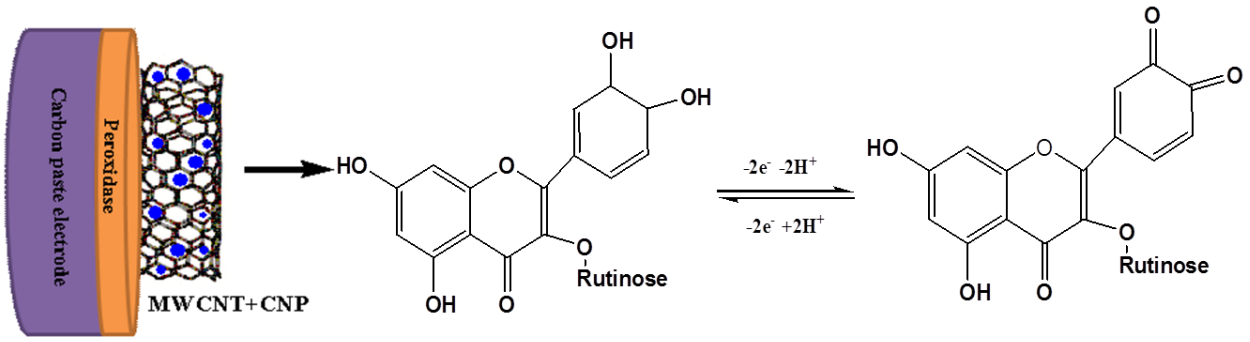

Figure 1. Schematic representation of the carbon paste electrode surface.

To optimize electrode composition, the concentration of components was varied according to Table 1.

The optimized POx/CeO_2/MWCNTs/CPE electrodes were prepared by hand mixing the carbon powder and other components in the optimal concentration described in Table 1, and after thoroughly rinsing the sensor with 0.1 mol L^{-1} phosphate buffer (pH 7.0), the electrodes were stored in the same buffer at 4 °C when not in use.

Table 1. Optimized biosensor parameters.

Biosensor parameters	Range studied	Optimal value
Graphite powder (% w/w)	60–75	75
Mineral oil (Nujol®) (% w/w)	40–25	25
Enzyme concentration (U/mg of carbon paste)	0.29-1.8	1.2
Cerium dioxide (mg)	1-5	2
Carbon nanotubes (mg)	0.1-2	1
H_2O_2 concentration (μmol L^{-1})	10-80	20

2.4. Electrochemical Measurements

Voltammetric experiments were carried out with a potentiostat/galvanostat μAutolab III® analysis system (Eco-Chemie, Utrecht, The Netherlands) integrated to GPES version 4.9® software. The measurements were performed in a 5.0 mL one-compartment electrochemical cell with a three-electrode system consisting of a carbon paste electrode, a Pt wire and the Ag/AgCl/KCl 3 mol L^{-1} (both purchased from Lab solutions, São Paulo, Brazil), representing the working electrode, the counter electrode and the reference electrode, respectively.

After optimizing the instrumental parameters of DPV and SWV, calibration curves were obtained by the successive addition of aliquots of the rutin stock standard solution into the electrochemical cell that already contained 5 mL of the supporting electrolyte; each concentration was

measured in six replicates. The experimental parameters for differential pulse voltammetry (DPV) were as follows: pulse amplitude = 50 mV, pulse width = 0.5 s and scan rate = 5 mV s^{-1}. The experimental parameters for cyclic voltammetry (CV) were as follows: scan rate = 100 mV s^{-1} and scan range was from 0.0 to 1.0 V vs. Ag/AgCl/KCl 3 mol L^{-1}. The DPV voltammograms were background subtracted and baseline corrected, and then all data were analyzed. All experiments were carried out at room temperature (25 ± 1 °C) in triplicate (n = 3), and the main electrolyte used was the 0.1 mol L^{-1} phosphate buffer solution (PBS) at pH (7.0). The electrolyte pH measurements were measured with a Mettler Toledo MA235 pH meter.

The microstructural characterization of the carbon paste electrode surface was performed using a scanning electron microscopy (SEM, JSM6701F, JEOL, Japan), and the transmission electron micrograph (TEM) images were obtained from a JEM-2010 HRTEM microscope (JEOL, Japan). The samples were dispersed in isopropyl alcohol under sonication and placed onto Cu grids (400 mesh, 3 mm diameter) used as sample holders

2.5 Optimization of the parameters for the electrochemical measurements by using the POx /CeO_2/MWCNTs/CPE electrode

Once the structure of the biosensor was defined, it was electrochemically optimized with respect to the accumulation potential, time and the pH effect.

2.5.1 Accumulation potential and accumulation time

The effect of the accumulation potential (E_{ac}) and accumulation time on the redox peak currents of rutin for the POx/CeO_2/MWCNTs/CPE electrode were studied from 0.0 to 1.0 V vs. Ag/AgCl/KCl, and the effect of accumulation time (t_{ac}) on the anodic peak current of rutin was evaluated by varying the time from 1 to 14 min.

2.5.2. Effect of pH on the performance of the biosensor

To determine the best pH value for the peroxidase catalyst, a series of buffer solutions were tested including Britton–Robinson at pH 4.0-5.0, acetate buffer at pH 3.0-6.0, phosphate buffer solution (PBS) at pH 7.0-8.0, ammonium–ammonia buffer at pH 8.0-11 and sulfuric acid solution at pH 2.0-4.0 under the same conditions at 0.1 mol L^{-1} as the supporting electrolyte in the electrochemical cell.

2.6 Studies of repeated reproducibility, storage stability and interferences of the POx /CeO_2/MWCNTs/CPE electrode

The optimized POx/CeO_2/MWCNTs/CPE electrodes prepared by hand mixing the components at the optimal concentration, as described in Table 1, were thoroughly washed with 0.1 mol L^{-1} phosphate buffer (pH 7.0) and stored in the same buffer at 4 °C when not in use.

The intra-day precision of the method was evaluated by repeating six experiments by DPV measurements in the rutin solution using the POx/CeO_2/MWCNTs/CPE. The inter-day precision of the determinations was investigated by measuring the current response of the modified electrode for six consecutive days using a solution 0.1 mol L^{-1} of the rutin. To assure the reproducibility, five different electrodes were used to determine the rutin concentrations.

In the studies of storage stability, the biosensor was stored in PBS at 8 °C, and the rutin measurements were carried out at after 10, 15, 20 and 30 days of storage. First, the biosensor was cleaned with voltammetric cycles in 0.1 mol L^{-1} PBS at pH 7.0 to eliminate the adsorbed rutin. After cleaning, the biosensor was used, and the results were expressed as the relative signal intensity, taken as 100% of the signal obtained during the first-day measurement.

Finally, the possible analytical applications of the proposed method and the effect of various substances as potentially electroactive interfering species were studied on the detection of rutin (0.1 mol L^{-1}).

2.7 Determination of rutin in pharmaceutical formulations

For verifying the applicability and reliability of the proposed method, pharmaceutical formulations (label amounts: 500 mg per tablet; 40 mg per capsule) were employed as standard samples for the determination of the rutin content. Five writing tablets and ten capsules were weighed, reduced to fine powder and mixed adequately. An accurate amount of the powder was weighed and extracted with 50 mL ethanol for 30 min in an ultrasonic bath. The solution was filtered into a 100-mL volumetric flask through ordinary filtration paper. Just before each measurement, the sample solution was diluted quantitatively using the supporting electrolyte. Six parallel determinations were performed.

2.8 Transmission electron microscopy (TEM) and scanning electron microscopy (SEM) images

High-resolution transmission electron microscopy (HRTEM) analyses were performed in the Microscopy Laboratory (LABMIC) at the Federal University of Goiás using a JEOL microscope (model JEM 2100) operating at 200 keV and with a resolution of 0.2 nm.

For analyses using scanning electron microscopy, the samples were fixed on glass supports and sputter coated with gold using a cathodic spraying process in a sputter coater - Desk V, Denton Vacuum. The secondary electron images (SEI) were acquired using a JEOL microscope, JSM-6610, operating at 10 kV and 20 kV.

3. RESULTS AND DISCUSSION

3.1 Electrochemical characterization of the different configurations of the CPE

Figure 2 shows the cyclic voltammetry curves recorded in the potential range from 0.0 to 0.6 V in a 0.1 mol L^{-1} pH 7.0 phosphate buffer solution (PBS) at a scan rate of 100 mV s^{-1}. The

electrochemical behavior of rutin on the different electrodes including a) bare CPE; b) POx/CPE; c) CeO_2/POx/CPE; d), MWCNT/POx/CPE and e) POx/CeO_2/MWCNTs/CPE was investigated.

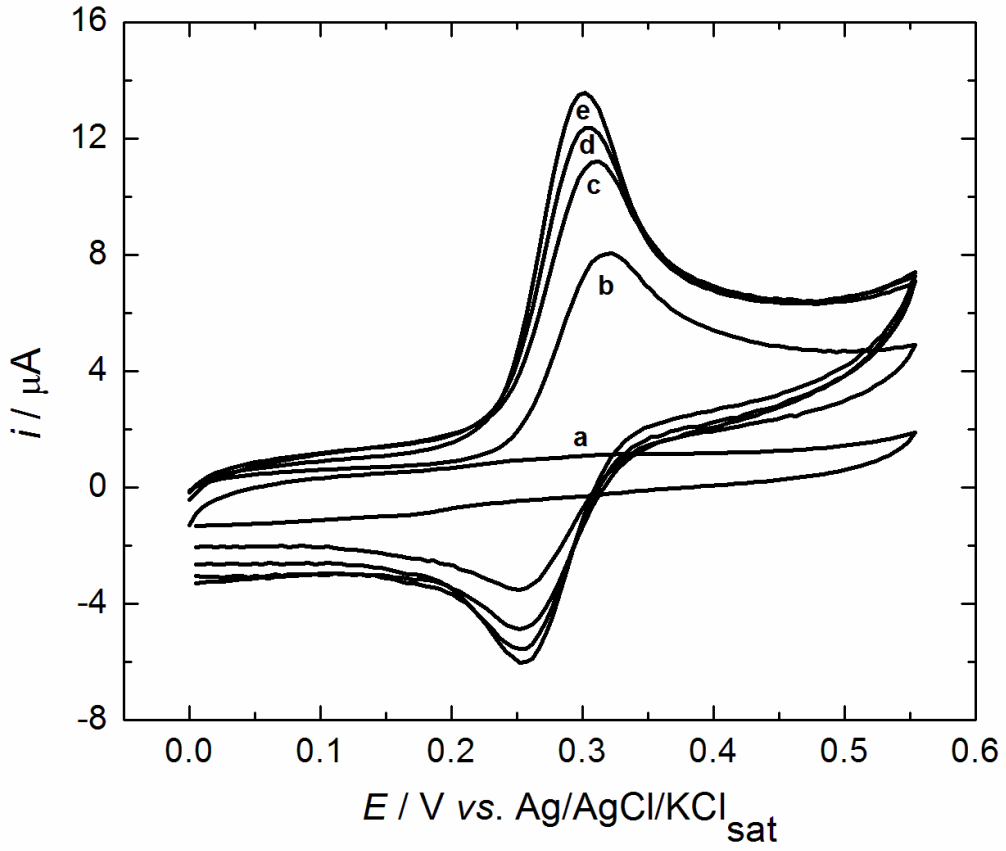

Figure 2. Cyclic voltammetric signals resulting from the electrochemical oxidation of 0.1 mol L^{-1} of rutin in a pH 7.0 PBS solution by using (a) CPE, (b) POx-CPE, (c) CeO_2-POx-CPE (d) MWCNT-POx-CPE, and (e) POx/ CeO_2/MWCNTs/CPE.

For all the different electrode configurations tested, a pair of redox peaks corresponding to the quasi-reversible electrochemical reaction of rutin was observed. Rutin is a flavonoid that contains four electroactive hydroxyl groups in its molecular structure, and its electrochemistry can be explained by a two-electron and two-proton redox process.

The bare electrode (curve-a) shows a low electrochemical response that may be due to the weaker adsorption of rutin on the electrode and/or slow electron transfer on the electrode surface. Moreover, a denaturation and loss of bioactivity of the enzyme can occur when there is a direct adsorption of POx onto the bare electrode surface [28].

The higher intensity currents for POx/CPE (curve-b) and CeO_2/POx/CPE (curve-c) electrodes demonstrate higher electrochemical performance for these two configurations compared with that of the bare CPE electrode. In the first case, POx increases significantly the peak intensity due to its enzymatic activity; later, the inclusion of CeO_2NPs reveals that nanoparticles increase the electroactive

surface of the electrode, resulting in improved electron transport properties between the analyte present in the electrolyte medium and the sensor surface.

However, modifying the POx/CPE electrode with MWCNTs, both the anodic and cathodic electrodes currents increase compared with those of the previous configurations, showing that the illustrative surface has significantly increased and hence the electron transfer has been improved, highlighting at the same time the quasi-reversible character of the redox process involving rutin (curve-d) [37].

Furthermore, the peak-to-peak potential separation as well as the current, slightly increased when the POx/CeO_2/MWCNTs/CPE was used. These findings could be attributed to the adequately higher electrocatalytic ability of the CeO_2NPs, which suggests that the modification of the POx-MWCNT-CPE electrode with these nanoparticles could be properly used for the quantification of rutin. The cathodic and anodic peaks appeared at 0.30 V and 0.25 V, respectively, with a ΔEp = 50 mV (curve-e).

After comparing the different electrodes, the response showed that the POx/CeO_2/MWCNTs/CPE obviously accelerates the redox reaction of rutin, which provides a slight shift of the anodic peak towards more negative potential values and significantly increases the anodic peak currents. The cathodic peak currents were also increased but to a lesser extent [36].

From Figure 2, it can be concluded that the modified CPE electrode is able to oxidize rutin at lower potentials (less positive) compared with the bare CPE, obtaining the lowest oxidation potential for the POx/CeO_2/MWCNTs/CPE electrode. This potential could be ascribed to the effective catalytic ability of the CeO_2NPs, which suggests that the mentioned electrode could be used as a sensor for the quantification of rutin. Moreover, the redox peak current was 10 times higher than that of the bare CPE, which indicated that the bare electrode was modified efficiently by the CNT-CeO_2 NPs nanocomposite.

3.2 Structural characterization of the CeO_2NPs - MWCNTs and POx enzyme materials

Once optimized, the structure of the biosensor and representative TEM images of the MWCNT with CeO_2 nanoparticle composites are shown in Figure 3A and Figure 3B at low and high magnification, respectively. It appears that the CeO_2 nanoparticles (hexagonal structure) were dispersed on the inner walls and external parts of the MWCNTs. The nanocomposite shows that the CeO_2 nanoparticles were agglomerated and anchored on the CNT surface with a size of 10–100 nm.

Furthermore, SEM images shown in Figure 4A, and Figure 4B reveals micron-sized particles formed by agglomeration of the CeO_2 nanoparticles. According to the micrographs, the nanocomposite is composed of these agglomerated CeO_2NPs surrounded by the MWCNTs. Figure 4B likewise demonstrates that the MWCNTs present a superstructure that shows a high degree of involvement in the accumulation of tubes. This finding can be represented by the report that MWCNTs allow for van der Walls interactions because their smooth, uniform surfaces are near each other. Subsequently, most of the tubes are packaged by means of direct van der Waals interactions along their entire length, and these results are in good agreement with previous reports [40].

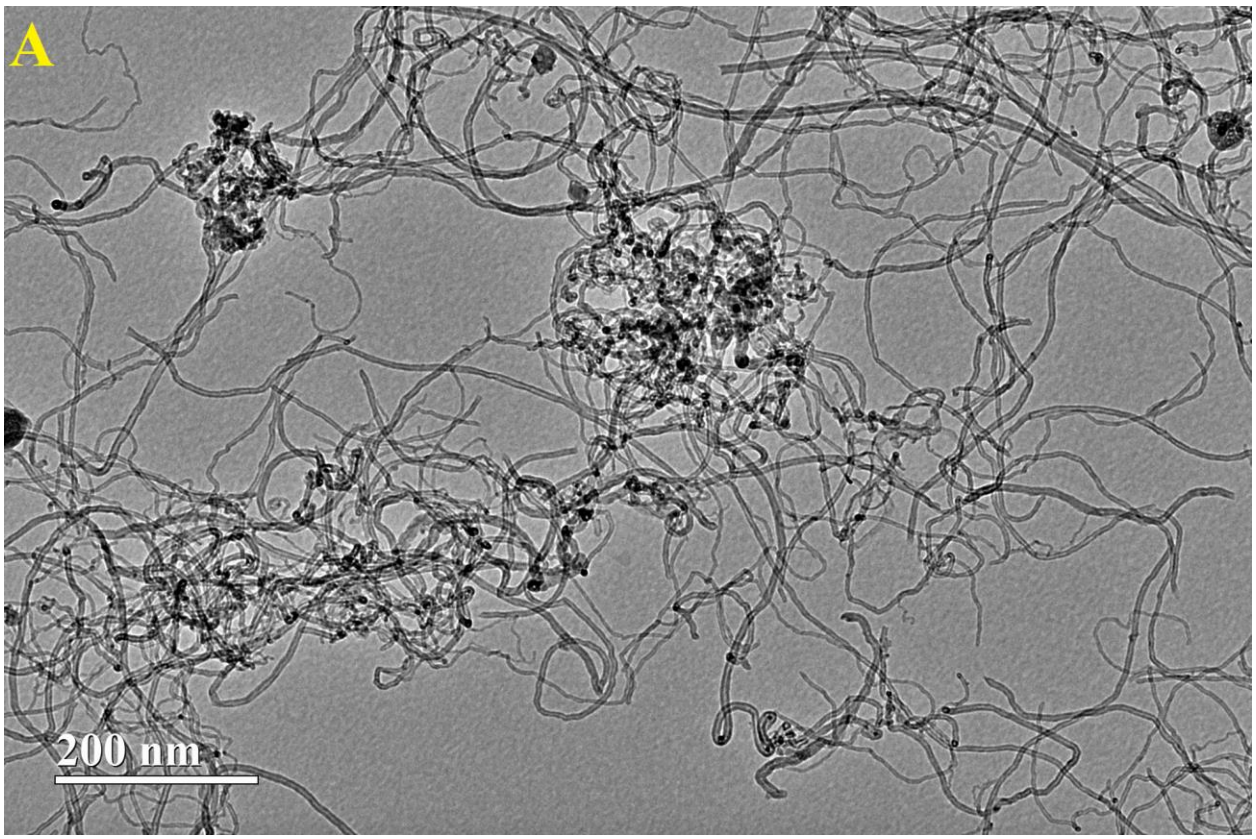

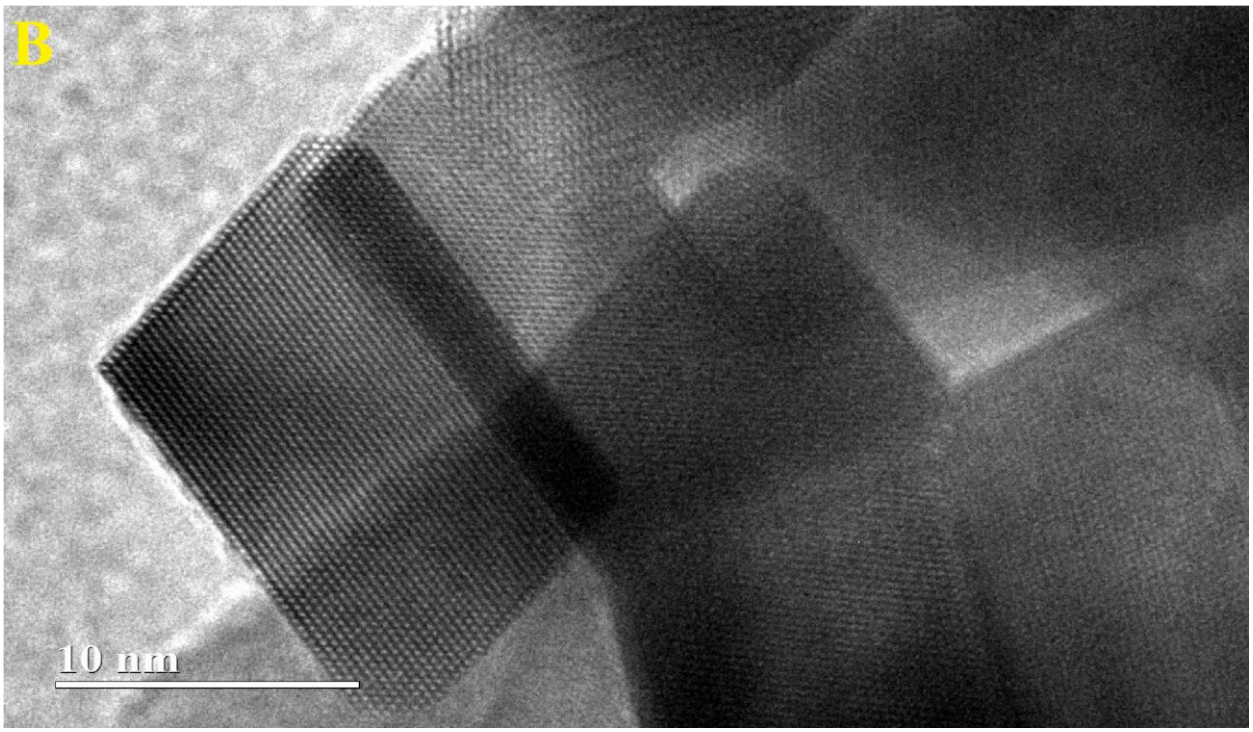

Figure 3. TEM images of the POx/CeO_2/MWCNTs/CPE: a) low magnification and b) high magnification.

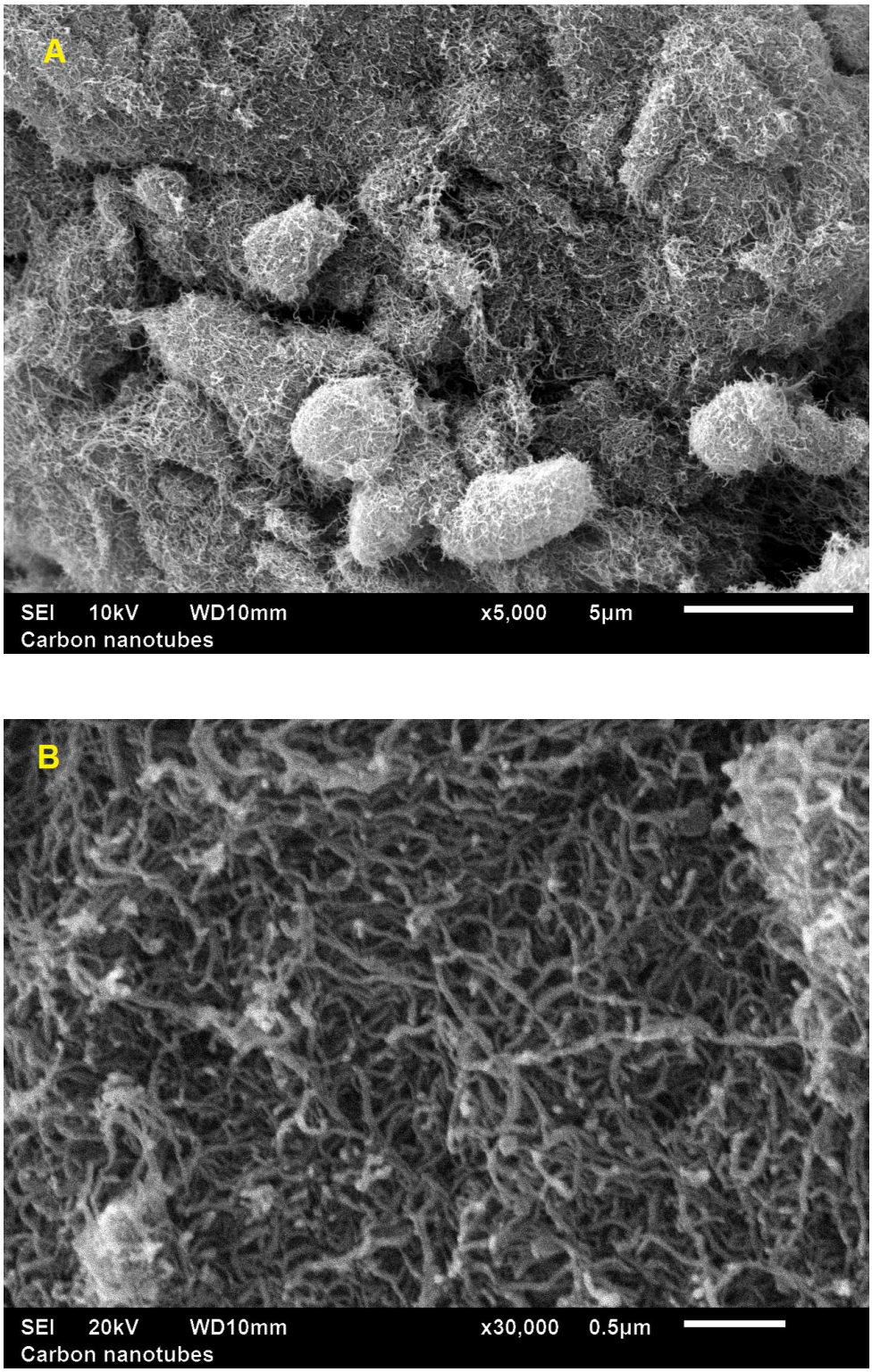

Figure 4. SEM images of the CeO_2NPs/CNT composite.

The surface morphologies of the POx/CeO_2/MWCNTs/CPE were studied by SEM, as shown in Figure 5. The SEM images at low and high magnifications in Figure 5A and Figure 5B, respectively, show that the electrode surface deeply changes in the presence of the POx crude extract. A comparison of the two images directly indicate that several biomolecules are adsorbed along the carbon nanotubes

and cerium oxide nanoparticles. The results show that the carbon nanotubes acted as a good adsorbent and as will be shown, as a good support for peroxidase immobilization.

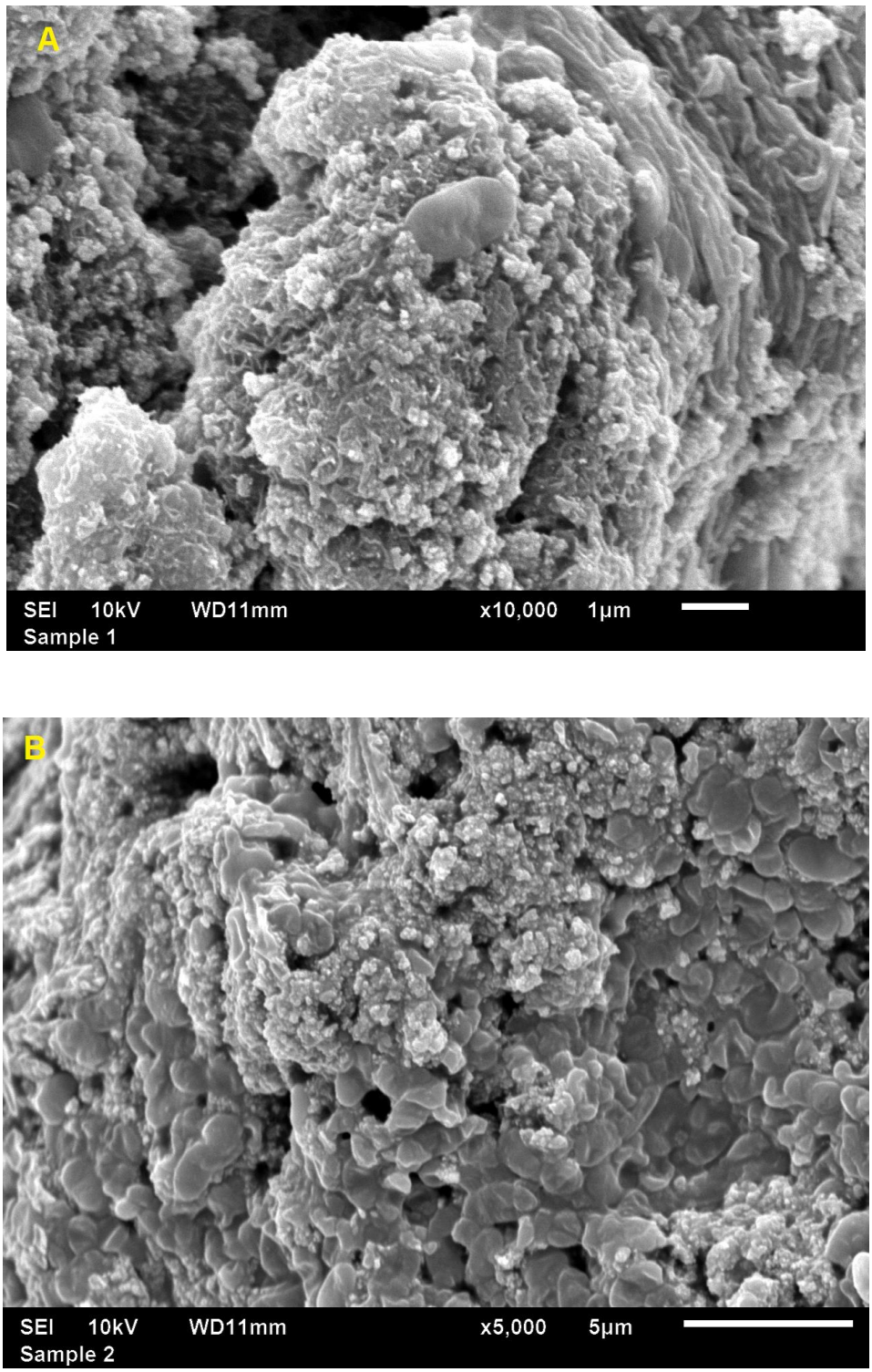

Figure 5. Low and high magnification SEM images of the POx/ CeO_2/MWCNTs/CPE (P. *cruentum-modified c*arbon paste electrode) composite.

3.3 Study of the electrochemical mechanism for the rutin redox process

The effect of scan rate on the electrocatalytic oxidation of rutin at a POx/CeO_2/MWCNTs/CPE was investigated by cyclic voltammetry.

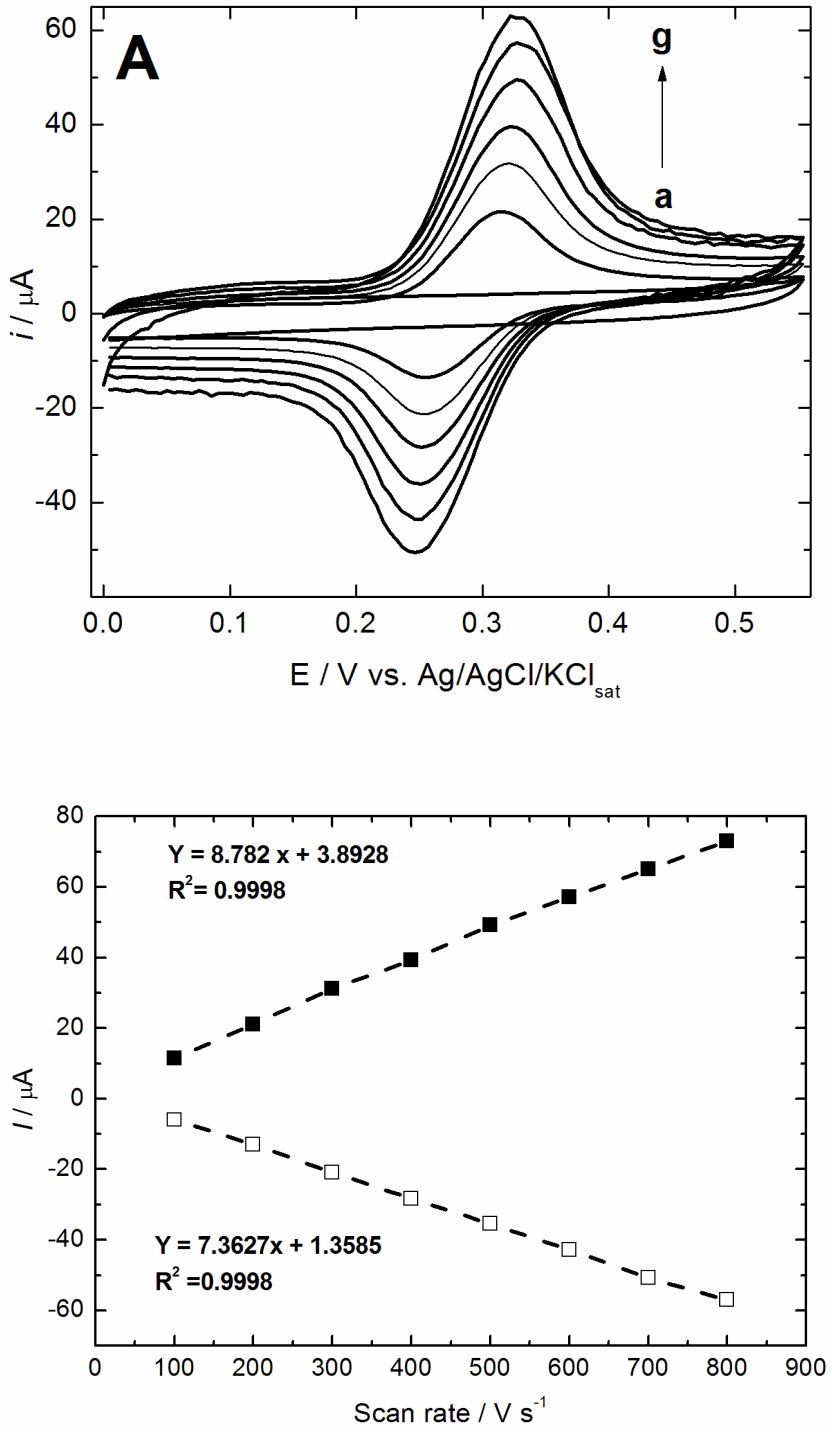

Figure 6. (A) Cyclic voltammograms obtained with 1 mmol L^{-1} of rutin in a 0.1 mol L^{-1} PBS buffer (pH 7.0) using the POx/CeO_2/MWCNTs/CPE electrode, (a–g) v = 100–700 mV s^{-1} at intervals of 100 mV·s^{-1}; and (B) plot of i_p vs. scan rate.

Figure 6A shows the cyclic voltammograms registered at different scan rates; the current peak of rutin oxidation increases linearly with the scan rate (v) in the range of 100–700 mV s^{-1}. Figure 6B shows that the current ratio between anodic and cathodic peaks (*Ipa* / *Ipc*) is very close to one at all scan rates used, which suggests that the electrocatalysis of rutin on the surface of the electrode proposed here is an adsorption - controlled process, as expected.

3.4. Optimization of the parameters for the electrochemical measurements by using a POx /CeO_2/MWCNTs/CPE electrode

3.4.1 Accumulation potential and accumulation time

The effect of the accumulation potential (E_{ac}) and accumulation time on the redox peak current of rutin for a POx/CeO_2/MWCNTs/CPE electrode was studied. Figure 7A and Figure 7B show the remarkable effect of the accumulation potential and accumulation time values during the oxidation of rutin.

The anodic peak current increased dramatically with a variation in the accumulation potential from 0.1 – 1.0 V, and then the current signal decreased gradually until a minimum value was reached at 1.0 V. Although, the POx/CeO_2/MWCNTs/CPE has an excellent response at lower voltages, the lower operating potential could minimize the interference from the matrix species and improve the linear response and sensitivity of the electrochemical sensor [41]. Thus, an accumulation potential of 0.2 V was chosen in subsequent experiments.

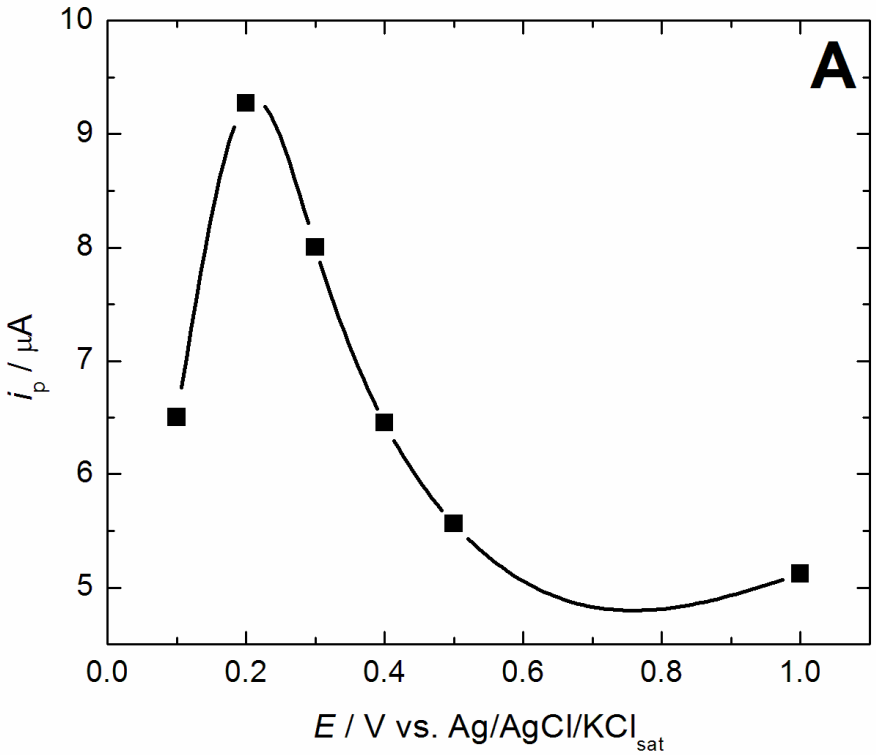

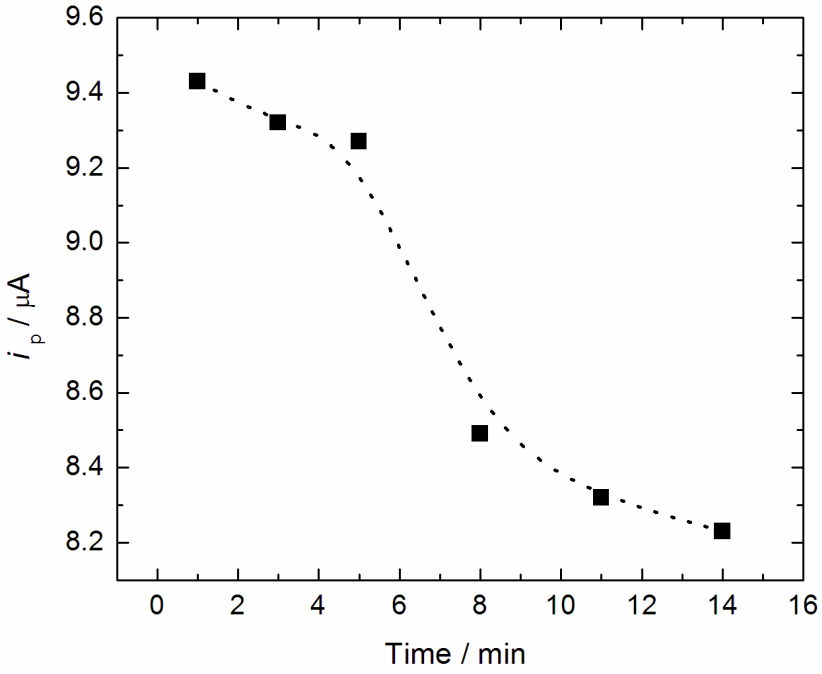

Figure 7. Effect of the accumulation potential (A) and accumulation time (B) on the oxidation peak current of 1 mmol L^{-1} of rutin at a POx/CeO_2/MWCNTs/CPE electrode in 0.1 mol L^{-1} of PBS solution at pH 7.0. The accumulation time for accumulation potential experiments was 200 mV.

Regarding the effect of the accumulation time (t_{ac}) on the anodic peak current of rutin, the greater times have lower peak currents, according to Figure 7B. When the accumulation time was approximately 1-14 min, a maximum in the peak current was obtained (for the 0.1 mol L^{-1} rutin solution). For higher time values, the current intensity levelled off and then decreased dramatically, which may be due to the saturation of the electrode surface. Therefore, 3 min was chosen as the accumulation time indicating that at this value for the POx/CeO_2/MWCNTs/CPE has a higher sensitivity towards H_2O_2.

3.4.2 Effect of pH

The response of the biosensor for rutin determination was recorded by using different buffer solutions. The investigation regarding the supporting electrolyte effect indicated that the phosphate buffer solution at pH 7 was the most suitable buffer system. Thus, to obtain the maximum sensitivity and enzymatic activity, the 0.1 mol L^{-1} PBS buffer in the pH 7 range, as shown in Figure 8, was selected for further experiments.

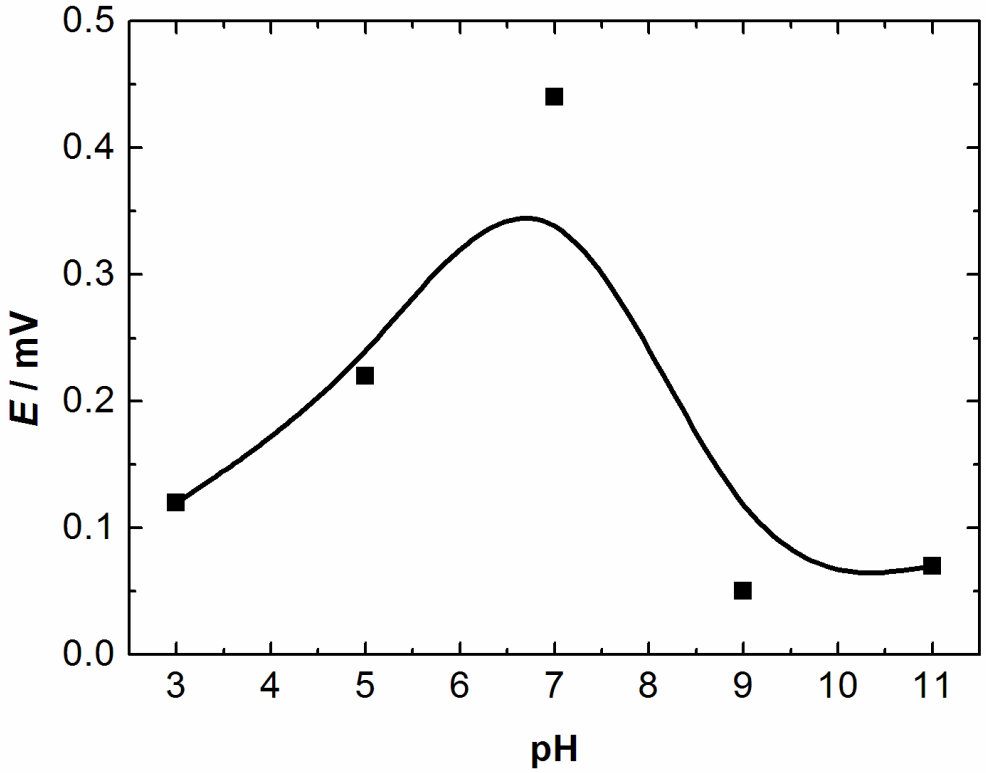

Figure 8. Response profile for the biosensor containing 0.1 mol L^{-1} of rutin in solutions with different pH values.

3.5 Determination of Rutin with a POx/CeO_2/MWCNTs/CPE electrode

By using the optimal formulation for the biosensor and the optimized parameters for the electrochemical measurements, DPV was explored for the determination of the electrocatalytic response of rutin.

Figure 9A shows typical DPV signals obtained at different concentrations of rutin. The peak currents show a good linear relationship with the rutin concentration in the range of $5\times10^{-7} - 8.0\times10^{-8}$ mol L^{-1}, as shown in Figure 9 B. The linear regression equation was I_{pa} = 2.5305[C_{Rutin}] (mol L^{-1}) + 4.7657 (R^2 = 0.9969); the limit of detection (LOD = 3(SD_a)/b) and limit of quantitation (LOQ = 10(SD_a)/b) were calculated as well, where SD_a is the standard deviation of the intercept and b is the slope of the calibration graph. The LOD and LOQ were found to be 0.3 and 0.9 µm of rutin, respectively, as described in Table 2. The analytical parameters of this electrode with other types of modified electrodes for rutin detection are compared and listed in Table 3 [42-49]. When looking at the values, the electrochemical performance and the results obtained with the POx/CeO_2/MWCNTs/CPE electrode proposed in this work for rutin determination are very similar and comparable to other sensors reported in the literature, but with the advantage of using an inexpensive POx crude extract. This method exhibits good linear range and, in some cases, the limits of detection for rutin is even lower.

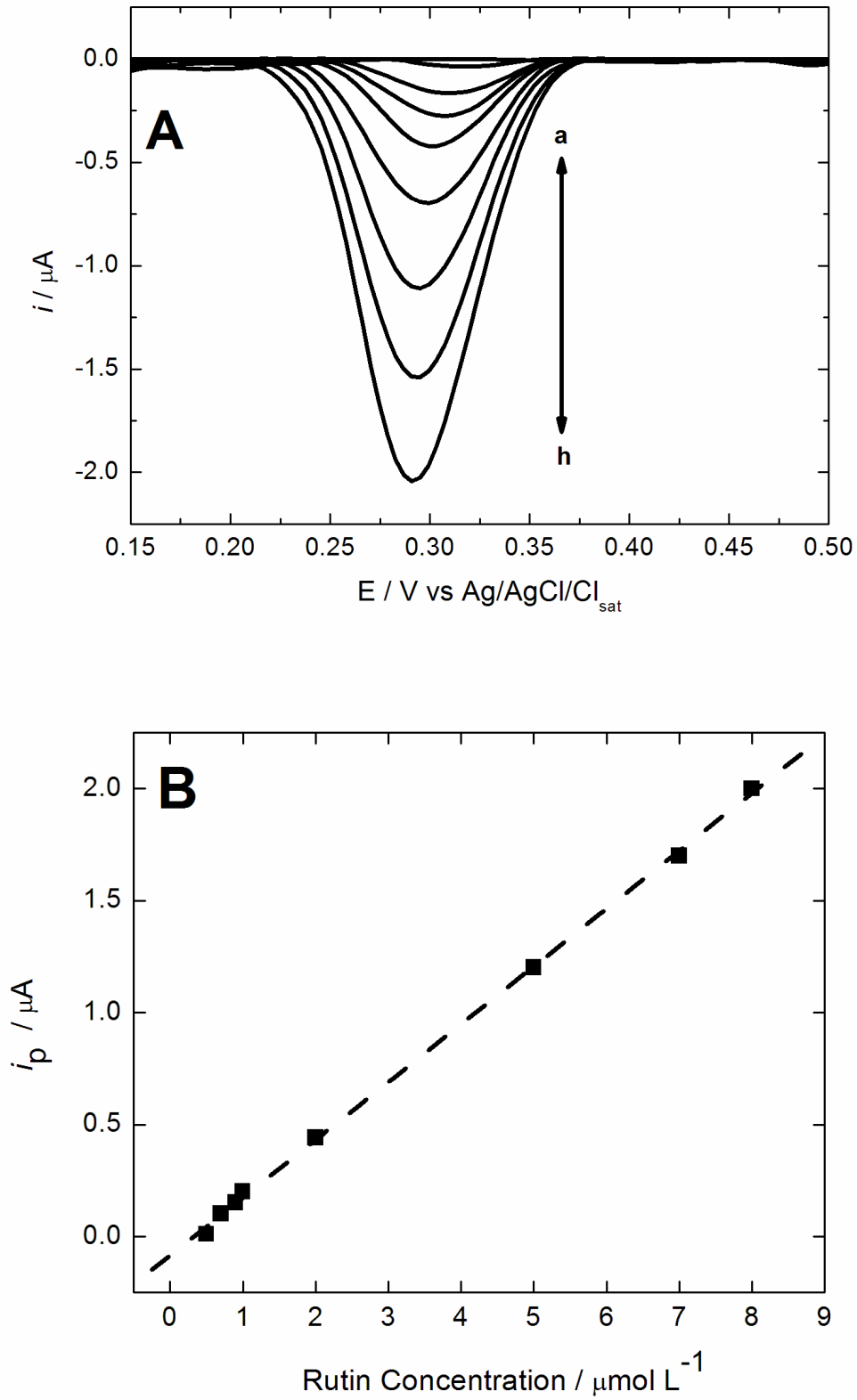

Figure 9. (A) Differential pulse voltammograms of POx / CeO_2/MWCNTs/CPE in 0.1 mol L^{-1} PBS (pH 7.0), pulse amplitude = 50 mV, scan rate = 10 mV s^{-1} with successive additions of rutin: (a) 0.5; (b) 0.7; (c) 0.9; (d) 1.0; (e) 2.0; (f) 5.0; (g) 7.0; and (h) 8.0 μmol L^{-1}. (B) The calibration curve for rutin.

Table 2. Analytical parameters for the determination of rutin using the POx/ CeO_2/MWCNTs/CPE biosensor.

Analytical Parameters	DPV	SWV
Peak potential	+0.28	
Correlation range (μmol L^{-1})	0.5-8.0	0.2-6.0
Regression equation	I_p = 2.5305 C + 4.7657	I_p = 1.4409 C + 3.54528
Regression coefficient	0.9969	0.9974
LOD (μmol L^{-1})	0.3	0.16
LOQ (μmol L^{-1})	0.9	0.4

Figure 10 A displays the square-wave voltammograms and the calibration curve obtained under the same optimized working conditions by using the proposed biosensor. The anodic peak current increased linearly with increasing rutin concentration in the range of $2 \times 10^{-7} – 6.0 \times 10^{-8}$ mol L^{-1}, as shown in Figure 10 B. The fitting equation was I_{pa} = 1.4409[*C*] (mol L^{-1}) + 3.5452 (R^2 = 0.9974), where i_p is the oxidative peak current in mA and C refers to the rutin concentration in mol L^{-1}, as described in the Table 2. The slopes of the two calibration plots are different due to the change in the accumulation efficiency and the different electroanalytical technique applied. Typically, SWV is more sensitive as DPV, as is confirmed from Figures 9 and 10. Moreover, for SWV, the LOD and LOQ values are lower than for DPV, as expected. Based on the signal-to-noise ratio of 3 (S/N), the detection limit is 0.16 μmol L^{-1} and limit of quantification is 0.4 μmol L^{-1} .

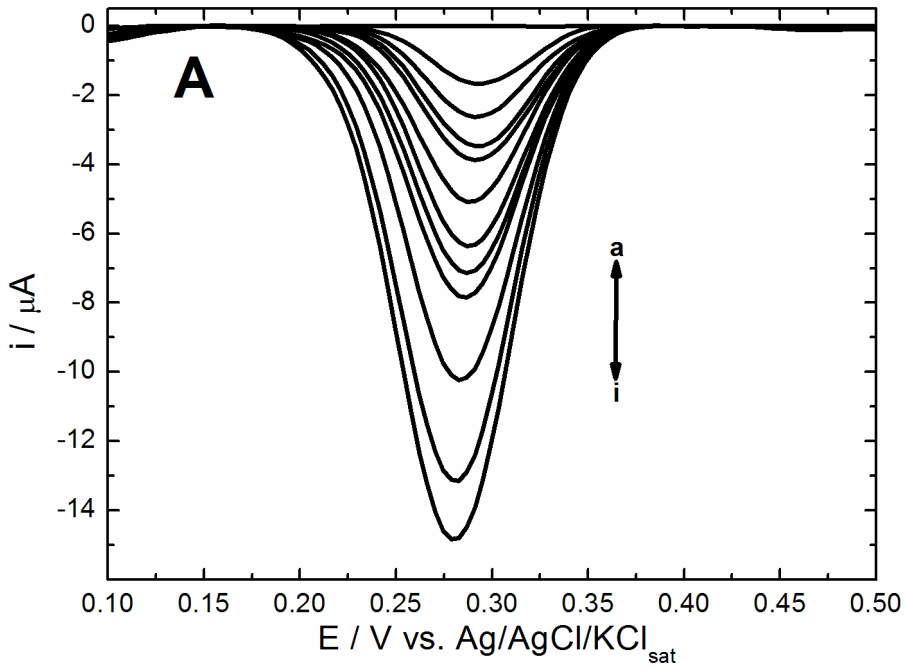

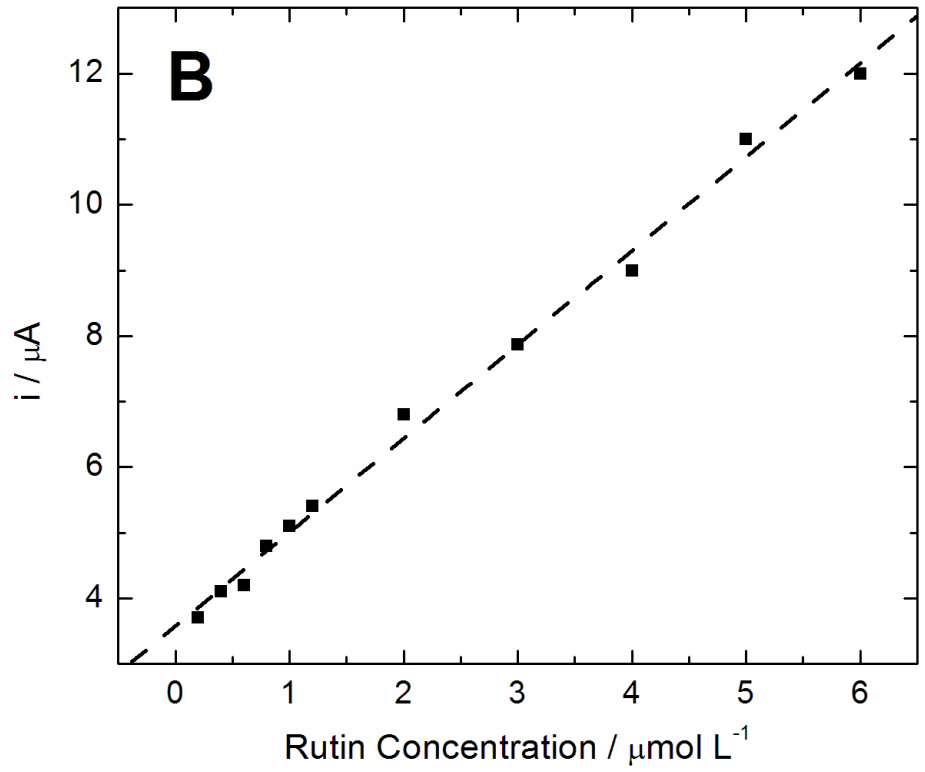

Figure 10 (A) Square-wave voltammograms of POx/ CeO_2/MWCNTs/CPE in 0.1 mol L^{-1} PBS (pH 7.0) with successive additions of rutin: (a) blank; (b) 0.2; (c) 0.4; (d) 0.5; (e) 0.7; (f) 1.0; (g) 1.2; (h) 2,0; (i) 3,0; (j) 4.0; (k) 5.0; and (i) 6.0 μmol L^{-1}. Frequency = 30 Hz, pulse amplitude = 50 mV and effective scan rate = 100 mV s^{-1} and (B) the calibration curve for rutin.

Table 3. Comparison of the analytical parameters for rutin detection with the proposed biosensor and various modified electrodes reported in the literature.

Electrode	Linear range μmol L^{-1})	Detection limit (μmol L^{-1})	Methods	Application	References
CNT/CPE	0.199 - 9.9	0.039	DPV	Tablets	[42]
IL [a] / CPE	0.5 - 100	0.35	CV	Tablets	[43]
MWCNT/ GCE	1.4 - 28 28 - 210	0.71	CV	Tablets	[44]
PABSA [b] / GCE	0.25 - 10	10	CV	Tablets	[45]
CNT/CPE	0.05 - 5	10	RDPV [c]	Capsules	[46]
AuNP-CD-LAC/CPE [d]	0.30-2.97	0.17	SWV	Capsule Cream	[47]
MWNTs/b-CD/GCE [e]	0.4-1000	0.20	CV	Urine	[48]
BMI-Tf_2 N-LAC/CPE [f]	4.77-46.2	0.45	SWV	Tablets	[49]
MWCNT/ CeO_2 /HRP/ CPE	0.5 - 8.0 0.2 - 6.0	0.3 0.16	DPV SWV	Tablets Capsules	This work

[a] IL-ionic liquid, [b] PABSA - poly(p-aminobenzene sulfonic acid), [c] RDPV- reverse differential pulse voltammetry, [d] AuNP-CD-LAC-gold nanoparticle-cyclodextrin-laccase, [e] b-CD-beta-cyclodextrin, and [f] Bmim-Tf_2N-1-butyl-3-methylimidazolium bis (trifluoromethyl sulfonyl) imide.

The analytical characterizations of the modified electrode show excellent reports for rutin determination at the surface of the proposed-modified electrode: POx/CeO_2/MWCNTs/CPE. The low limit of detection of the biosensor can be attributed to several factors such as the large surface area of the POx/CeO_2/MWCNTs/CPE, better adsorption of rutin, and electrocatalytic effects of the nanomaterials used as modifiers. Considering the adsorption of rutin, the poor electronic conductivity of CeO_2 is enhanced with the CNT support to facilitate the charge transfer rate. This real expanded conductivity and the added surface area in the CNT/CeO_2 composite increases its usage by free electron conduction between the interface of the oxide and the conducting CNTs. Consequently, the combination of the CNT and CeO_2 in the nanocomposite electrode resulted in a higher capacitance compared with the individual components.

3.6 Repeatability, Reproducibility, Stability (RSD) and Interferences of the modified electrode

The intra-day precision of the developed method (DPV) for rutin solution was evaluated by replicate analysis (n = 6) using the POx/CeO_2/MWCNTs/CPE and was determined to be very high. The RSD value of the current peak was found to be 1.09%, indicating excellent repeatability of the modified electrode. The relative standard deviation for the inter-day precision was 1.27% for six successive days using same concentration of rutin. The RSD of 1.5% (n = 6) was estimated using six different electrodes successively.

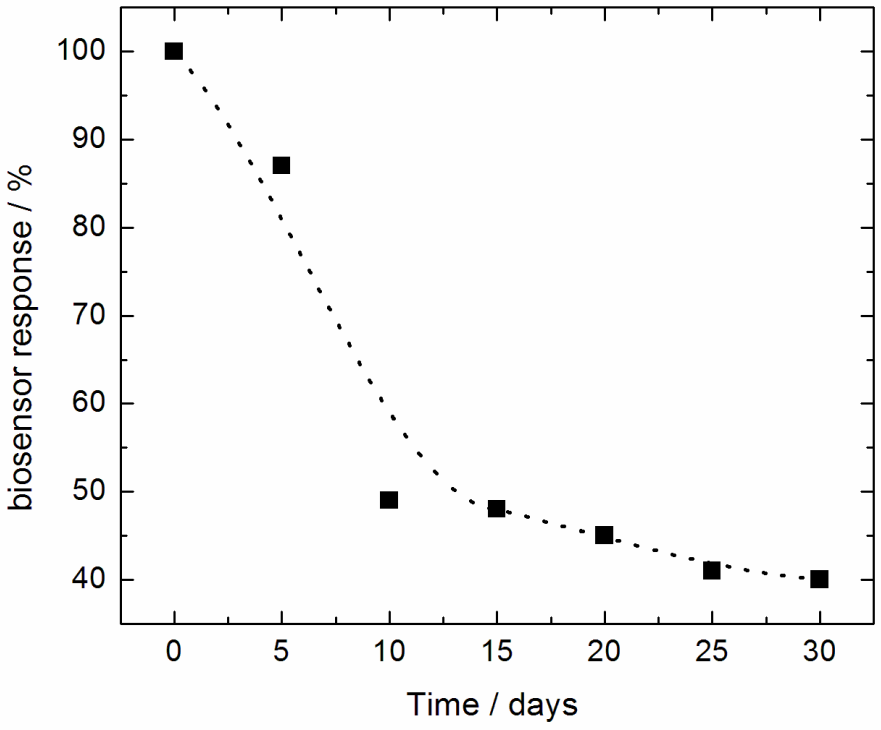

Figure 11. Stability of the biosensor.

Table 4. Recovery studies in Rutin capsules determined by the proposed biosensor.

Sample	Rutin determined by proposed method		
	Expected (μmol L^{-1})	Found(μmol L^{-1}) [a]	Recovery (%)
Capsule	1	0.98 ± 0.07	98.74
	3	2.97 ± 0.04	97.28
	5	5.1 ± 0.01	102.52
Tablet	1	0.99± 0.06	99.74
	3	2.98± 0.01	98.58
	5	5.0± 0.03	100.68

[a] Averages and standard deviations (SDs) of the six replicate determinations.

The results of the storage stability of proposed biosensor are given in Figure 11. The current response decreased approximately 2% in 1 week, while after 30 days of storage the electrode maintained 15% of the signal. The decrease in the signal intensity during long-term stability of this proposed biosensor is relatively satisfactory. Thus, the good stability, reproducibility and repeatability of the method at the modified electrode have been demonstrated. These results indicate that HRP/CeO_2/MWCNTs/CPE could be used for rutin analysis.

Finally, none of the tested compounds or ions had an interference effect on the peak currents of rutin, even after the addition of a 100-fold excess of the material, suggesting that the proposed method has good selectivity for the determination of rutin.

3.7 Determination of rutin in pharmaceutical formulations

Table 5. Determination of rutin in real samples.

Drug Sample (mg)	Label Concentration	Content of rutin found by DPV (mg) ± SD [a]	Recovery (%)	RSD[b] (%)
Tablet 1	0.5 g/tablet	500.6 ± 2.10	100.12	1.66
Capsule	0.04 g/capsule	0.040 ±2.22	100.6	1.56

[a]Averages and standard deviations (SDs) of the six replicate determinations.

[b]RSD: relative standard deviations also calculated for the six replicates.

For verifying the applicability and reliability of the proposed method, pharmaceutical formulations were employed as standard samples for the determination of the rutin content. The results

obtained in the POx/CeO_2/MWCNTs/CPE are listed in Table 4. After the determination, some standard rutin solution was added into the solution and the recovery was re-detected (Table 5). The recovery determination of the rutin content was between 97.28% and 102.52% and showed good agreement with the label value. These results confirmed that the present method possessed good precision and accuracy for determination of rutin.

4. CONCLUSIONS

In this study, a carbon paste electrode modified with cerium dioxide nanoparticles, POx enzyme and multiwall carbon nanotubes was used for the sensitive and selective voltammetric determination of rutin. The modified electrode can be used as an electrochemical method for the determination of rutin. The cerium dioxide and carbon nanotubes effectively facilitate the electrocatalysis of rutin and the electron transfer on the electrode surface. These materials also increase the sensitivity of the sensor, which shows good linearity as a function of concentration. The capability of the modified electrode in terms of selectivity, linearity, limit of detection, quantification, and repeatability are comparable with the analytical parameters of other reported modified electrodes. In addition, the POx/CeO_2/MWCNTs/CPE offers some advantages over traditional electrodes including stability and reproducibility. We have also shown the effectiveness of the modified electrode by testing its ability to determine the presence of rutin in pharmaceutical samples (tablets and capsules) with very good percentages of recovery.

ACKNOWLEDGMENTS
The authors thank Conselho Nacional de Desenvolvimento Científico e Tecnológico (CNPq), Grant no. 554569/2010-8, Coordenação de Aperfeiçoamento de Pessoal de Nível Superior (CAPES) and Fundação de Amparo à Pesquisa do Estado de Goiás (FAPEG) for financial support. We would also like to thank Tatiane Oliveira dos Santos from the Microscopy Laboratory (LABMIC) of the Federal University of Goiás, Goiânia, Brazil for the acquisition of electron microscopy images.

References

1. A. Wojdyło, J. Oszmiański, and R. Czemerys, *Food Chem*, 105 (2007) 940.
2. S. Kumar and A.K. Pandey, *Sci World J,* 2013 (2013) 1.
3. A. García-Lafuente, E. Guillamón, A. Villares, M.A. Rostagno, and J.A. Martínez, *Inflamm Res*, 58 (2009) 537.
4. O. Benavente-Garcı, F.R. Marin, A. Ortun, and J. Del Rio, *J Agric Food Chem*, 45 (1997) 4505.
5. R. Christov, and V. Bankova, *J Chromatogr A*, 623 (1992) 182.
6. L. Duan, L. Yang, H. Xiong, X. Zhang, and S. Wang, *Microchim Acta*, 180 (2013) 355.
7. H. Xu, Y. Li, H. W. Tang, X. K. Hao, and W. Qiong-Shui, *Anal Lett*, 43 (2010) 893.
8. S.K. Vashist, D. Zheng, K. Al-Rubeaan, J.H. Luong, and F.S. Sheu, *Biotechnol Adv*, 29 (2011) 169.

9. L. Kong, and W. Chen, *Adv Mater*, 26 (2014) 1025.
10. V.V. Mody, R. Siwale, A. Singh, and H.R. Mody, *J Pharm Bioallied Sci*, 2 (2010) 282.
11. E.E.S. Bruzaca, I.C. lopes, E.H.C. Silva, P.A.V. Carvalho, A.A. Tanaka, *Microchem J*, 133 (2017) 81.
12. A.T. Lawal, *Mater Research Bulletin*, 73 (2016) 308.
13. T.A. Silva, F.C. Moraes, B.C. Janegitz and O. Fatibello-Filho, *J Nanomaterials*, 2017 (2017) 1.
14. S.G. Shruthi, C.V. Amitha and B.B. Mathew, *J Instrument Technology*, 2 (2014) 26.
15. P. Nayak, P.N. Santhosh, and S. Ramaprabhu, *J Nanosci Nanotechnol*, 15 (2015) 4855.
16. C.I.L. Justino, A.R. Gomes, A.C. Freitas, A.C. Duarte, and T.A.P Rocha-Santos, *Trends in Analytical Chem*, 91 (2017) 53.
17. Y. Zhang and Q Wei, *J Electroanal Chem*, 781 (2016) 401.
18. A. Hayat, G. Catanante, and J.L. Marty, *Sensors*, 14 (2014) 23439.
19. Z. Zhu, L. Garcia-Gancedo, and A. J. Flewitt, *Sensors*, 12 (2012) 5996.
20. M. Diaconu, S. C. Litescu, and G.L. Radu, *Sensors Actuators B Chem*, 145 (2010) 800.
21. E.F.M. Gabriel, P.T. Garcia, T.M.G. Cardoso, F.M. Lopes, F.T. Martins, and W.K.T. Coltro, *Analyst*, 141 (2016) 4749.
22. S.A. Eremia, V. Vasilescu, and A. Radoi, *Talanta*, 110 (2013) 164.
23. N.C. Veitch, *Phytochemistry*, 65 (2004) 249.
24. A.C. Pereira, A. Kisner, C.R.T. Tarley, N. Durán, and L.T. Kubota, *Dynam Biochem Process Biotechn and Molecular Biology*, 3 (2009) 75.
25. E. Ferapontova, and E. Puganova, *J Electroanal Chem*, 518 (2002) 20.
26. R.S. Freire, C.A. Pessoa, L. D. Mello, and L. T. Kubota, *J Braz Chem Soc*, 14 (2003) 230.
27. R. Mohammad, M. Ahmad, and L.Y. Heng, *Sensor and Actuat* 241 (2017) 141.
28. Z. Wang, M. Li, and P. Su, *Electrochem Commun*, 10 (2008) 306.
29. P. Brugnerotto, T.R. Silva, D. Brondani, E. Zapp, and I.C Vieira, *Electroanalysis* 29 (2017) 1037.
30. K. Thenmozhi, and S.S. Narayanan, *Mater Sci and Engineering C*, 70 (2017) 223.
31. J. Wang, G. Liu, M.R. Jan, and Q. Zhu, *Electrochem Commun*, 5 (2003) 1000.
32. T. Ruzgas, E. Csöregi, J. Emnéus, L. Gorton, and G. Marko-Varga, *Anal Chim Acta*, 330 (1996) 123.
33. I.C. Vieira, K.O. Lupetti, and O. Fatibello-Filho, *Quim Nova*, 26 (2003) 39.
34. K.O. Lupetti, L. Ramos, I.C. Vieira, and O. Fatibello-Filho, *II Farmaco*, 60 (2005) 179.
35. R.S. Freire, C.A. Pessoa, L.D. Mello, and L.T. Kubota, *J. Braz. Chem. Soc.* 14 (2003) 230.
36. I.Gul, M.S. Ahmad, S.M.S. Naqvi, A. Hussain, R. Wali, A.A. Farooqi, and I Ahmed, *J App Biology & Biotechnol*, 5 (2017) 072.
37. W. Feng, and P. Ji, *Biotechnol Adv*, 29 (2011) 889.
38. O. Fatibello-Filho, and I.C. Vieira, *Quim Nova* 25 (2002) 455.
39. F. Colmati, S.A. Yoshioka, V.L. Silva, H. Varela, and E.R. Gonzalez, *Int J Electrochem Sci* 2 (2007) 195.
40. M.J. O'Connell, P. Boul, and L. M. Ericson, *Chem Phys Lett*, 342 (2001) 265.
41. Z. Wang, M. Li, and P. Su, *Electrochem Commun* 10 (2008) 306.
42. A.C. Oliveira, and L.H. Mascaro, *Curr Anal Chem*, 7 (2011) 101.
43. W. Sun, M. Yang, and Y. Li, *J Pharm Biomed Anal*, 48 (2008) 1326.
44. G. Ziyatdinova, I. Aytuganova, and A. Nizamova, *Collect Czechoslov Chem Commun* 76 (2011) 1619.
45. X. Chen, Z. Wang, and F. Zhang, *Chem Pharm Bull*, 58 (2010) 475.
46. X.Q. Lin, J.B. He, and Z.G. Zha, *Sensors Actuators, B Chem*, 119 (2006) 608.
47. P. Brugnerotto, T.R. Silva, D. Brondani, E. Zapp, and I.C. Vieira, *Electroanalysis*, 29 (2017) 1031.
48. J-L. He, Y. Yang, X. Yang, Y-L. Liu, Z-H. Liu, G-L. Shen, and R-Q. Yu, *Sensors Actuators B Chem*, 114 (2006) 94.

49. A.C. Franzoi, P. Migowski, J. Dupont, I. C. Vieira, *Anal Chim Acta*, 639 (2009) 90.

© 2018 The Authors. Published by ESG (www.electrochemsci.org). This article is an open access article distributed under the terms and conditions of the Creative Commons Attribution license (http://creativecommons.org/licenses/by/4.0/).